Journal of Ceramic Processing Research. Vol. 15, No. 6, pp. 371~375 (2014)

J O U R N A L O F
Ceramic Processing Research

Simultaneous synthesis and consolidation of nanostructured WSi_2-$NbSi_2$ composite by pulsed current activated heating and its mechanical properties

Hyoung-Gon Jo and In-Jin Shon*

Division of Advanced Materials Engineering, Research Center of Advanced Materials Development, Chonbuk National University, 664-14 Deokjin-dong 1-ga, Deokjin-gu, Jeonju, Jeonbuk 561-756, Korea

Nanopowders of W, Nb, and Si were fabricated by high-energy ball milling. A dense nanostructured WSi_2-$NbSi_2$ composite was simultaneously synthesized and sintered by the pulsed current activated heating method within four minutes using mechanically activated powders of W, Nb, and Si. A high-density WSi_2-$NbSi_2$ composite was produced under simultaneous application of an 80-MPa pressure and a pulsed current. The sintering behavior, mechanical properties, and microstructure of the composite were investigated.

Key words: Composite, Mechanical properties, Sintering, Nanostructured materials.

Introduction

WSi_2 and $NbSi_2$ have been investigated as potential materials for high-temperature structural applications and for use in the electronics industry. Their properties provide a desirable combination of a high melting temperature, high modulus, good oxidation resistance in air, a relatively low density [1], and the ability to undergo plastic deformation above 1200 °C [2]. However, as in the case of many similar compounds, the current concern about these materials (WSi_2 and $NbSi_2$) focuses on their low fracture toughness below the ductile-brittle transition temperature [3, 4]. To improve the mechanical properties of these materials, the fabrication of a nanostructured material and composite material [5-8] have been found to be effective. As nanomaterials possess high strength, high hardness, excellent ductility and toughness, undoubtedly, more attention has been paid to their potential application [9, 10].

Recently, nanocrystalline powders have been produced by high-energy milling [11-13]. The sintering temperature of high-energy mechanically milled powder is lower than that of unmilled powder due to the increased reactivity, internal and surface energies, and surface area of the milled powder, which contribute to its so-called mechanical activation [14-16]. The grain size in sintered materials becomes much larger than that in pre-sintered powders due to rapid grain growth during a conventional sintering process. Therefore, controlling grain growth during sintering is one of the keys to the commercial success of nanostructured materials. In this regard, the pulsed current activated sintering method (PCASM), which can make dense materials within 2 minutes, has been shown to be effective in achieving not only rapid densification to near theoretical density, but also the prohibition of grain growth in nanostructured materials [17-20].

This paper reports on the rapid synthesis and consolidation of dense nanostructured WSi_2-$NbSi_2$ composite starting with high-energy ball-milled nanopowders. The mechanical properties, sintering behavior and grain sizes of the resulting nanostructured WSi_2-$NbSi_2$ composite were also evaluated.

Experimental Procedures

Powders of 99.8% pure Nb (−325 mesh, Alfa Products), 99.5% pure Si (−325 mesh, Aldrich Products), and 99.8% pure W (0.5 μm, Daegu Tec. Product) were used as starting materials. 0.5W, 0.5Nb, and 2Si powder mixtures were first milled in a high-energy ball mill (Pulverisette-5 planetary mill) at 250 rpm and for 10 h. Tungsten carbide balls (9 mm in diameter) were used in a sealed cylindrical stainless steel vial under an argon atmosphere. A charge ratio (ratio of ball mass to powder) of 30 : 1 was used. The grain size was calculated using Suryanarayana and Grant Norton's formula [21]:

$$B_r\,(B_{crystalline}+B_{strain})\cos\theta = k\,\lambda / L + \eta\sin\theta \qquad (1)$$

where B_r is the full width at half-maximum (FWHM) of the diffraction peak after an instrumental correction; $B_{crystalline}$ and B_{strain} are the FWHM caused by the grain size and internal stress, respectively; k is a constant (with a value of 0.9); λ is the wavelength of the X-ray

*Corresponding author:
Tel : +82-63-270-2381
Fax: +82-63-270-2386
E-mail: ijshon@chonbuk.ac.kr

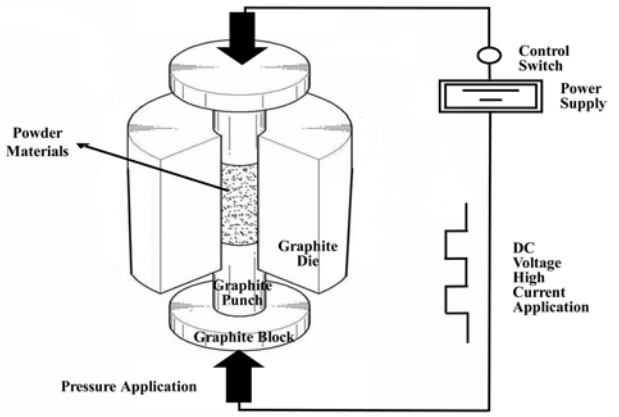

Fig. 1. Schematic diagram of the pulsed current activated sintering apparatus.

radiation; L and η are the grain size and internal strain, respectively; and θ is the Bragg angle. The parameters, B and B_r, follow the Cauchy's form with the relationship $B = B_r + B_s$, where B and B_s are the FWHM of the broadened Bragg peaks and the standard Bragg peaks of the samples, respectively.

After milling, the powder was placed in a graphite die (outside diameter = 35 mm, inside diameter = 10 mm, and height = 40 mm), and then introduced into the pulsed current-activated sintering system, shown schematically in Fig. 1. The four major stages in the synthesis are as follows: evacuation of the system to 40 mtorr (stage 1), application of a uniaxial pressure of 80 MPa (stage 2), activation of a pulsed current, which was maintained until densification was attained as indicated by a linear gauge measuring the shrinkage of the sample (stage 3), and cooling the sample to room temperature (stage 4). Temperatures were measured by a pyrometer focused on the surface of the graphite die. The process was carried out under a vacuum of 40 mtorr (5.3 Pa).

The relative densities of the sintered samples were measured by the Archimedes method. Microstructural information was obtained from product samples, which were polished and etched for 1 minute at room temperature using a solution composed of HF (10 vol.%), HNO_3 (30 vol.%), and H_2O (60 vol.%). Compositional and microstructural analyses of the products were made through X-ray diffraction (XRD) and scanning electron microscopy (SEM) with energy dispersive X-ray analysis (EDAX). Vickers hardness was measured by performing indentations with a load of 5 kg and a dwell time of 15 s on the synthesized samples.

Results and Discussion

Fig. 2 shows XRD pattern of SEM images of milled 0.5W-0.5Nb-2Si powders. Only W, Nb, and Si peaks were observed, as marked. Therefore, it is obvious that no chemical reaction occurred between the component powders during milling. Nevertheless, the peaks of the powders are significantly wide, suggesting that their

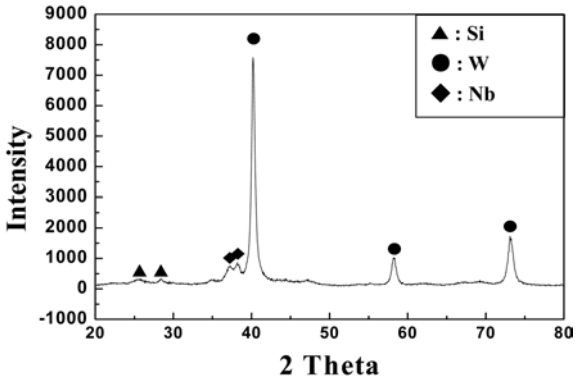

Fig. 2. XRD pattern of 0.5W-0.5Nb-2Si powder milled for 10 h.

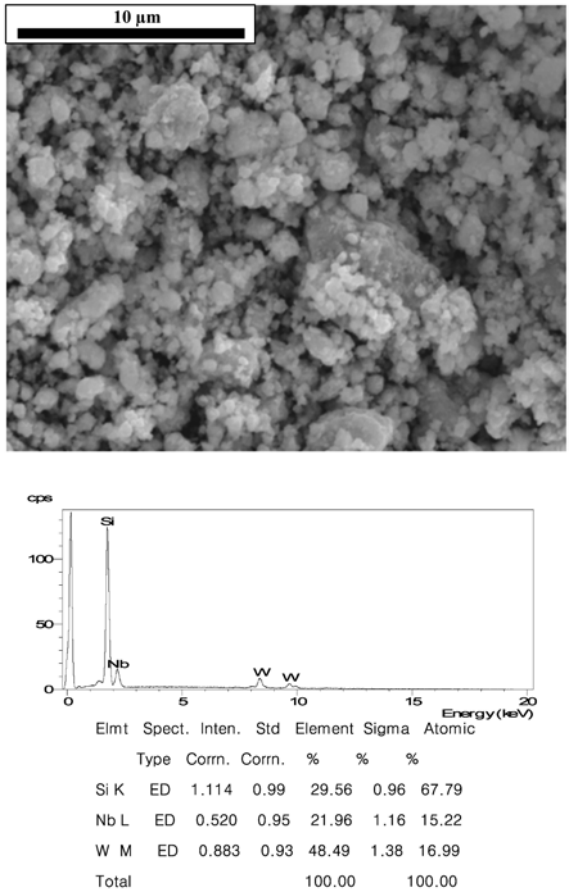

Fig. 3. SEM image and EDS of 0.5W-0.5Nb-2Si powder milled for 10 h.

grain sizes became very fine due to the milling. The average grain size of W measured by Suryanarayana and Grant Norton's formula [21] was about 22 nm. SEM image of milled powders, and EDS analysis were shown in Fig. 3. The milled powders have a very fine grain size and some agglomeration. In EDS, only W, Nb, and Si peaks were detected. The milling process is known to introduce impurities from the ball and/or container. However, in this study, peaks of Fe was not identified.

The variations in shrinkage displacement and tem-

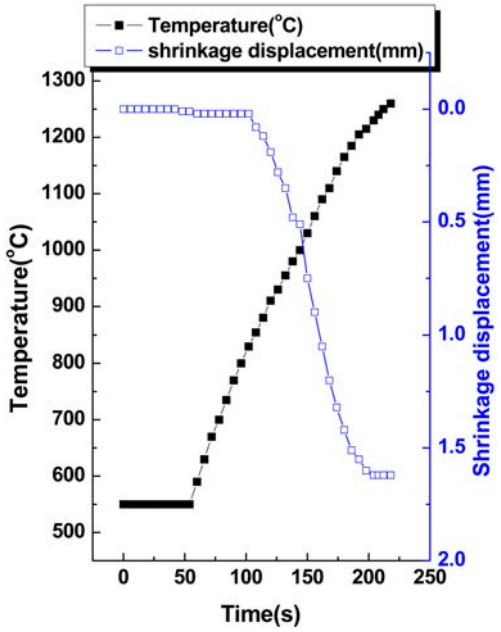

Fig. 4. Variations of temperature and shrinkage displacement with heating time during synthesis and densification of the $0.5WSi_2$-$0.5NbSi_2$ composite.

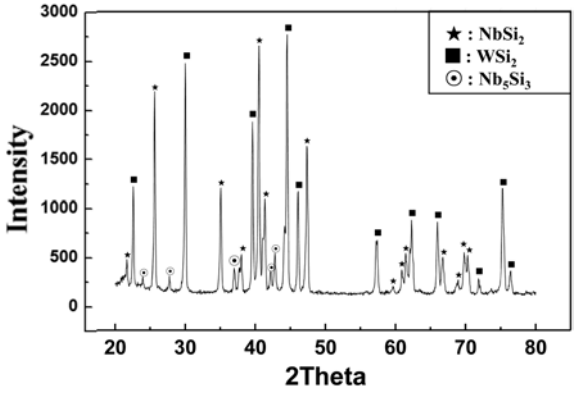

Fig. 5. XRD patterns of the 0.5Nb-0.5W-2Si system heated at 1250 °C.

perature of the surface of the graphite die upon heating during the synthesis and densification of $0.5WSi_2$-$0.5NbSi_2$ composite are shown in Fig. 4. As the pulsed current was applied, the shrinkage displacement was nearly constant with temperature up to 800 °C, and then abruptly increased. Fig. 5 shows the X-ray diffraction result of the sample heated to 1250 °C. The reactant peaks of W, Nb, and Si were not detected and product peaks of WSi_2 and $NbSi_2$ were observed**.** And minor phase (Nb_5Si_3) observed by X-ray diffraction analyses, as show in Fig. 5. The presence of Nb_5Si_3 of the sample suggests a deficiency of Si. It is considered that this observation is related to entrapped oxygen in the pores of the interior portion of the sample during pressing or maybe due to a little oxidation of Si during the heating. The interaction between these phases, i.e.,

$$0.5W + 0.5Nb + 2Si \rightarrow 0.5WSi_2 + 0.5NbSi_2 \quad (2)$$

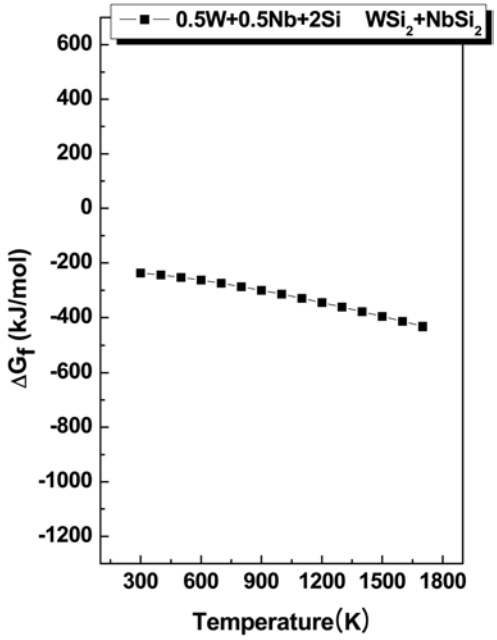

Fig. 6. Temperature dependence of the Gibbs free energy change by interaction of the 0.5W + 0.5Nb + 2Si.

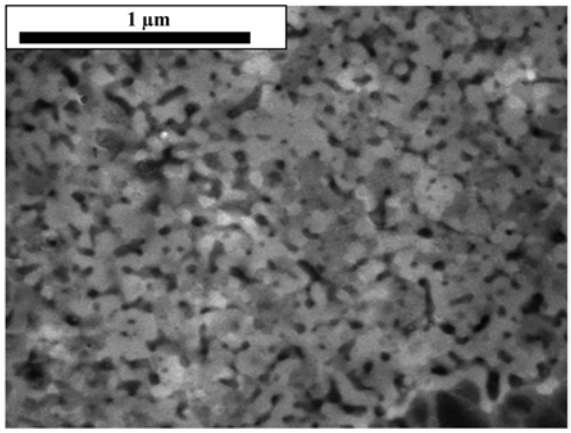

Fig. 7. FE-SEM image of $0.5WSi_2$-$0.5NbSi_2$ composite sintered at 1250 °C.

is thermodynamically feasible, as shown in Fig. 6.

The abrupt increase in the shrinkage displacement at the ignition temperature is due to the increase in density resulting from the change in the molar volume associated with the formation of WSi_2 and $NbSi_2$ from the reactants (W, Nb, and Si) and the consolidation of the product.

The average grain size of WSi_2 and $NbSi_2$ measured by Suryanarayana and Grant Norton's formula [21] was about 125 and 131 nm, respectively. A FE-SEM image of the etched surface of the sample heated to 1250 °C under a pressure of 80 MPa is shown in Fig. 7. The microstructure consists of nanophases in the FE-SEM image. The corresponding relative density is 96%. The role of the current during sintering and/or synthesis has been the focus of several attempts to provide an explanation for the observed sintering enhancement and

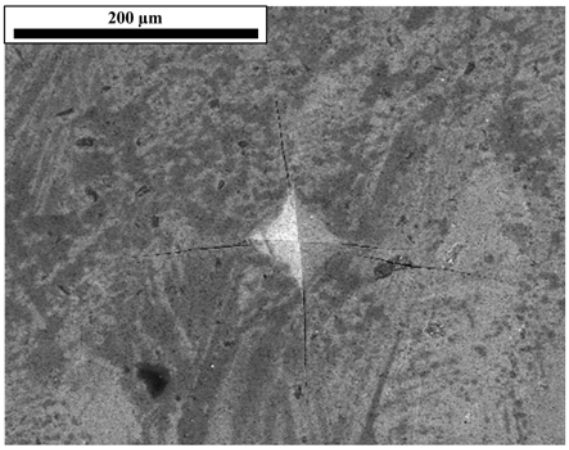

Fig. 8. Vickers hardness indentation in the $0.5WSi_2$-$0.5NbSi_2$ composite.

the improved product characteristics. The role played by the current has been broadly interpreted by several groups. The effect has been explained by rapid heating due to Joule heating at contacts points, the presence of plasma in pores separating powder particles, and the intrinsic contribution of the current to mass transport [22-25].

Vickers hardness measurements were made on polished sections of the $0.5WSi_2$-$0.5NbSi_2$ composite using a 10-kg load and 15-s dwell time. The calculated hardness value of the $0.5WSi_2$-$0.5NbSi_2$ composite was 1218 kg/mm^2. This value represents an average of five measurements. Indentations with large enough loads produced median cracks around the indentations. The length of these cracks permits an estimation of the fracture toughness for the material. From the length of these cracks, fracture toughness values can be determined using the formula developed by Anstis *et al*. [26], which is

$$K_{IC} = 0.016\ (E/H)^{1/2} \cdot P/C^{3/2} \quad (3)$$

where E is Young's modulus, H is the indentation hardness, P is the indentation load, and C is the trace length of the crack measured from the center of the indentation. The modulus was estimated by the rule of mixtures for the 0.478 volume fraction of WSi_2 and the 0.522 volume fraction of $NbSi_2$ using $E(WSi_2) = 468$ Gpa [27] and $E(NbSi_2) = 363$ Gpa [25]. As in the case of hardness values, the toughness values were derived from the average of five measurements. The toughness value obtained by this method of calculation is 3.5 MPa $\cdot$ m$^{1/2}$. These fracture toughness and hardness values of the nanostructured $0.5WSi_2$-$0.5NbSi_2$ composite are higher than those (fracture toughness; 3.2 MPa $\cdot$ m$^{1/2}$ hardness; 8.2 Mpa) of the microstructured WSi_2 [3] or those (fracture toughness; 2.5 MPa $\cdot$ m$^{1/2}$ hardness; 876 kg/mm^2) of the nanostructured $NbSi_2$ [4]. The enhanced hardness and fracture toughness of WSi_2-$NbSi_2$ composite is believed that $NbSi_2$ and WSi_2 in the composite may deter the propagation of cracks and $NbSi_2$ and WSi_2 have nanostructure phases. A typical indentation pattern for the $0.5WSi_2$-$0.5NbSi_2$ composite is shown in Fig. 8. Typically, one to three additional cracks were observed to propagate from the indentation corner.

Conclusions

W, Nb and Si nanopowders were fabricated using high-energy ball milling for 10 h. Using the pulsed current activated sintering method, a $0.5WSi_2$-$0.5NbSi_2$ composite was simultaneously synthesized and consolidated using the mechanically activated powders of 0.5W, 0.5Nb, and 2Si within four minutes. The relative density of the composite was 96% for the applied pressure of 80 MPa. The average grain sizes of WSi_2 and $NbSi_2$ in $0.5WSi_2$-$0.5NbSi_2$ composite sintered by this method were determined as 125 and 131 nm, respectively.

The average hardness and fracture toughness values obtained were 1218 kg/mm^2 and 3.5 MPa $\cdot$ m$^{1/2}$, respectively. The enhanced hardness and fracture toughness of WSi_2-$NbSi_2$ composite is believed that $NbSi_2$ and WSi_2 in the composite may deter the propagation of cracks and $NbSi_2$ and WSi_2 have nanostructure phases.

Acknowledgments

This research was supported by the Basic Science Research Program, through the National Research Foundation of Korea (NRF), funded by the Ministry of Education (No. 2012R1A1A4A01001300) and this work was supported by the Human Resources Development program (No. 20134030200330) of the Korea Institute of Energy Technology Evaluation and Planning (KETEP) grant funded by the Korea government Ministry of Trade, industry and Energy.

References

1. A.K. Vasudevan, J.J. Petrovic, Mater Sci Eng. A 155, (1992) 1-17.
2. R. Mitra, Y.R. Mahajan, N.E. Prasad, W.A. Chiou, C. Ganguly. Key Eng Mater. 108-110, (1995) 11-16.
3. I.J. Shon, D.h. Rho, H.C. Kim, Metals and Materials, 6 (2000) 533-538.
4. I.Y. Ko, B.R. Kim, K.S. Nam, B.M. Moom, B.S.Lee, I.J. Shon, Met. Mater. Int., 15, (2009) 399-403.
5. I.J. Shon, I.Y. Ko, H.S. Kang, K.T. Hong, J.M. Doh, J.K. Yoon, Met. Mater. Int., 18, (2012) 115-119.
6. Y. Ohya, M. J. Hoffmann, G. Petzow, J Am Ceram Soc. 75, (1992) 2479-2483.
7. S. K. Bhaumik, C. Divakar, A. K. Singh, G. S. Upadhyaya, J Mater Sci Eng. A 279, (2000) 275-281.
8. I.J. Shon, K.I. Na, J.M. Doh, H.K. Park, J.K. Yoon, Met.Mater. Int., 19, (2013) 99-103.
9. H.S. Nalwa, Hanbook of Nanostructured Materials and Nanotechnology. Academic Press, Tokyo, 1996.
10. S. Berger, R. Porat, R. Rosen, Progress in Materials

Science 42, (1997) 311-320.
11. G.W. Lee, I.J. Shon, Korean J. Met. Mater. 51, (2013) 95-100.
12. I.J. Shon, G.W. Lee, J.M. Doh, J.K. Yoon, Electronic Materials Letters, 9, (2013) 219-225.
13. I.J. Shon, G.W. Lee. J.M. Doh, J.K. Yoon, Journal of Ceramic Processing Research 14 (2013) 292-296.
14. F. Charlot, E. Gaffet, B. Zeghmati, F. Bernard, J. C. Liepce, Mater. Sci. Eng. A 262, (1999) 279-278.
15. W. Kim, C.Y. Suh, K.M. Roh, S.W. Cho, K.I Na, I.J. Shon, Journal of Alloys and Compounds 568 (2013) 73-77.
16. M.K. Beyer, H. Clausen-Schaumann, Chem. Rev. 105, (2005) 2921-2948.
17. I.J. Shon, K.I. Na, J.M. Doh, H.K. Park, J.K. Yoon, Met. Mater. Int. 19 (2013) 99-103.
18. Na-Ra Park, Kwon-Il Na, Hanjung Kwon, Jae-Won Lim, and In-Jin Shon, Korean J. Met. Mater. 51 (2013) 753-759.
19. S.M. Kwak, H.K. Park, I.J. Shon, Korean J. Met.Mater., 51, (2013) 314-348.
20. I.J. Shon, S.L. Du, J.M. Doh, J.K. Yoon, Met. Mater. Int. 19, (2013) 1041-1045.
21. C. Suryanarayana, M. Grant Norton, X-ray Diffraction A Practical Approach, Plenum Press, New York (1998).
22. Z. Shen, M. Johnsson, Z. Zhao and M. Nygren, J. Am. Ceram. Soc. 85, (2002) 1921-1927.
23. J. E. Garay, U. Anselmi-Tamburini, Z. A. Munir, S. C. Glade and P. Asoka- Kumar, Appl. Phys. Lett. 85, (2004) 573-575.
24. J. R. Friedman, J. E. Garay. U. Anselmi-Tamburini and Z. A. Munir, Intermetallics. 12, (2004) 589-597.
25. J. E. Garay, J. E. Garay. U. Anselmi-Tamburini and Z. A. Munir, Acta Mater., 51, (2003) 4487-4495.
26. G.R. Anstis, P. Chantikul, B.R. Lawn, D.B. Marshall, J. Am. Ceram. Soc. 64, (1981) 533-538.
27. F. Chu, M. Lei, S. A. Maloy. J.J. Petrovic, T.E. Mitchell. Acta mater. 44, (1996) 3035-3048.